

Managing for ecological surprises in metapopulations

Supplemental materials

Kyle Logan Wilson¹, Colin Bailey¹, William Atlas¹, and Doug Braun²

¹*Earth to Ocean Research Group, Simon Fraser University*

²*Fisheries & Oceans Canada*

04 July 2019

Metapopulation model

Local & metapopulation dynamics

Our metapopulation is defined by a set of local populations N_p for a species with a one year generation time with time-dynamics that follows birth (i.e., recruitment R), immigration, death, and emigration (BIDE) processes:

$$N_{it+1} = R_{it}\epsilon_{it} + I_{it} - D_{it} - E_{it}$$

where N_{it+1} is the number of adults in patch i at time t , R_{it} is number of recruits, I_{it} is number of recruits immigrating into patch i from any other patch, D_{it} is number of recruits that die due to disturbance regime, E_{it} is the number of recruits emigrating from patch i into any other patch, and ϵ_{it} is stochasticity in recruitment.

Resource monitoring often occurs at the scale of the metapopulation, hence we define metapopulation adults as:

$$MN_t = \sum_{i=1}^{N_p} N_{it}$$

with metapopulation recruits:

$$MR_t = \sum_{i=1}^{N_p} R_{it}$$

Local patch recruitment at time t depended on adult densities at $t-1$ and followed a reparameterized Beverton-Holt function:

$$R_{it} = \frac{\alpha_i N_{it-1}}{1 + \frac{\alpha_i - 1}{\beta_i} N_{it-1}}$$

where α_i is the recruitment compensation ratio and β_i is local patch carrying capacity.

Management often monitors metapopulation resources as the aggregate of all local populations. For example, take a two patch metapopulation model that varies α_i and β_i parameters where:

```
alpha <- c(2, 4)
beta <- c(100, 200)
```

Here, recruitment compensation from local patches α_i gets averaged across the metapopulation leading to an average compensation ratio $\bar{\alpha}$ of 3. Likewise, the total carrying capacity of the metapopulation $\bar{\beta}$ becomes the summation of local patch carrying capacities $\sum \beta_i$, which is 300. This scale of monitoring generates the following local patch and metapopulation dynamics:

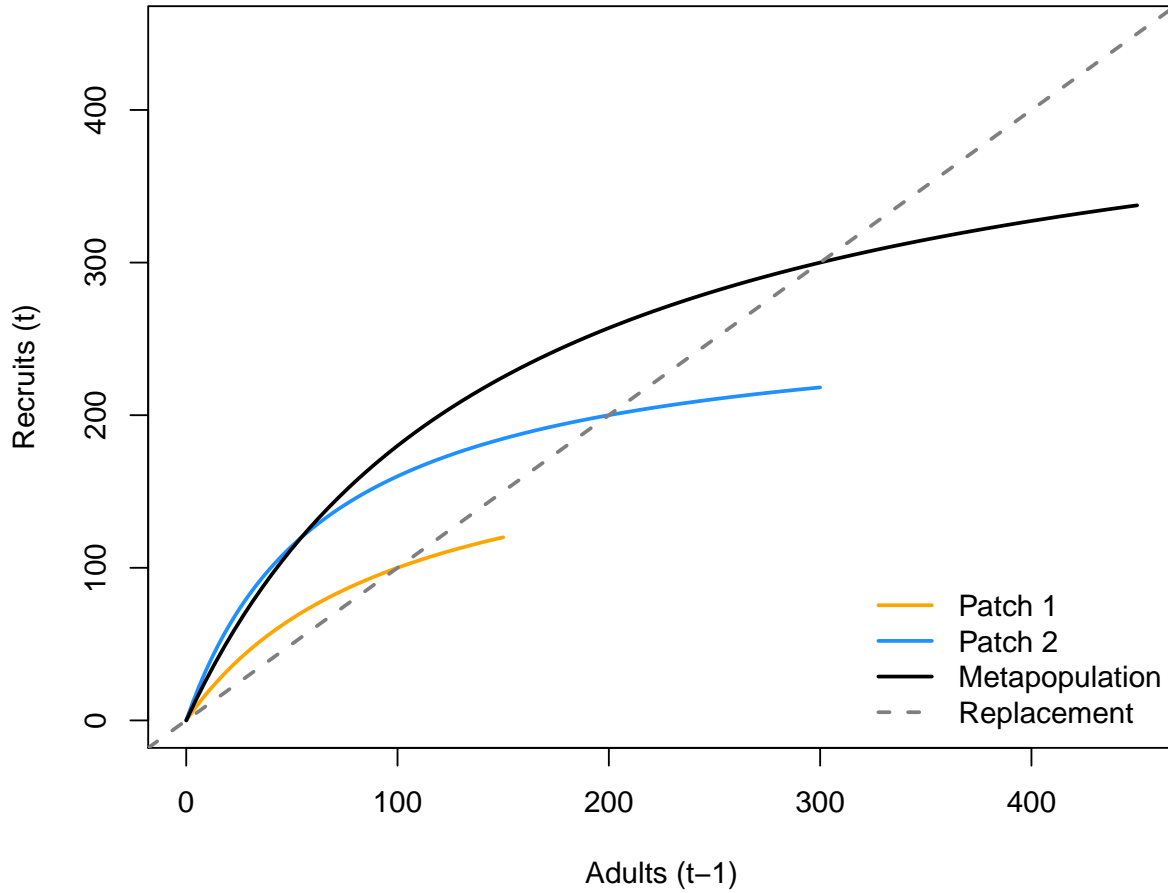


Figure S1: Metapopulation and local patch recruitment dynamics.

Creating the spatial networks

The next aspect to our metapopulation model is connecting the set of patches to one another. We need to specify the number of patches, their arrangements (i.e., connections), and how far apart they are from one another. We followed some classic metapopulation and source-sink arrangements to create four networks that generalize across a few real-world topologies: a linear habitat network (e.g., coastline), a dendritic or branching network (e.g., coastal rivers), a star network (e.g., mountain & valley, or lake with inlet tributaries), and a complex network (e.g., terrestrial plants).

To make networks comparable, each spatial network type needs the same leading parameters (e.g., number of patches N_p and mean distance between neighboring patches \bar{d}). In this case, we set N_p to 16 and \bar{d} to 1 unit (distance units are arbitrary). We used the `igraph` package and some custom code to arrange our spatial networks as the following:

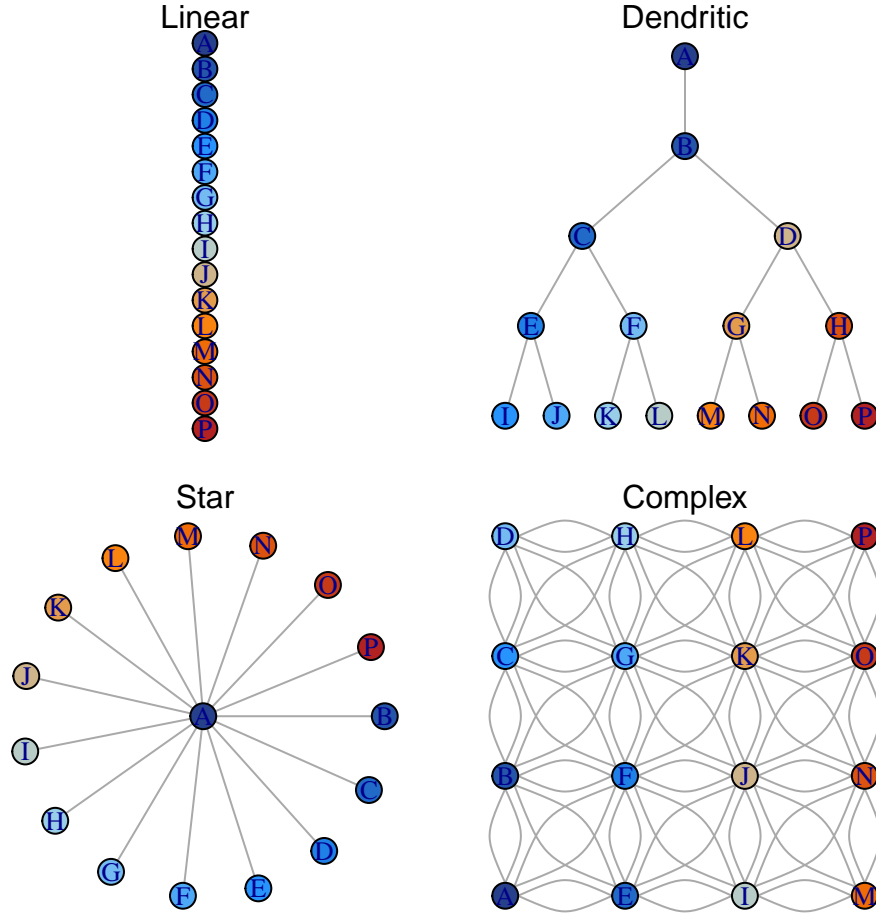


Figure S2: Four spatial network topologies.

44 Note that distances between neighbor patches in the above networks are equal.

45 An example dispersal matrix for the complex network:

46	##	A	B	E	F	C	G	D	H	I	J	K	L	M	N	O	P
47	##	A	0	1	1	1	2	2	3	3	2	2	2	3	3	3	3
48	##	B	1	0	1	1	1	1	2	2	2	2	2	2	3	3	3
49	##	E	1	1	0	1	2	2	3	3	1	1	2	3	2	2	2
50	##	F	1	1	1	0	1	1	2	2	1	1	1	2	2	2	2
51	##	C	2	1	2	1	0	1	1	1	2	2	2	2	3	3	3
52	##	G	2	1	2	1	1	0	1	1	2	1	1	1	2	2	2
53	##	D	3	2	3	2	1	1	0	1	3	2	2	2	3	3	3
54	##	H	3	2	3	2	1	1	1	0	3	2	1	1	3	2	2
55	##	I	2	2	1	1	2	2	3	3	0	1	2	3	1	1	2
56	##	J	2	2	1	1	2	1	2	2	1	0	1	2	1	1	1
57	##	K	2	2	2	1	2	1	2	1	2	1	0	1	2	1	1
58	##	L	3	2	3	2	2	1	2	1	3	2	1	0	3	2	1
59	##	M	3	3	2	2	3	2	3	3	1	1	2	3	0	1	2
60	##	N	3	3	2	2	3	2	3	2	1	1	1	2	1	0	1
61	##	O	3	3	2	2	3	2	3	2	2	1	1	1	2	1	0
62	##	P	3	3	3	2	3	2	3	2	3	2	1	1	3	2	1

Dispersal

Dispersal from patch i into patch j depends on constant dispersal rate ω (defined as the proportion of total local recruits that will disperse) and an exponential distance-decay function between i and j with distance cost to dispersal m following:

$$E_{ij(t)} = \omega R_{it} p_{ij}$$

where E_{ij} is the total dispersing animals from patch i into patch j resulting from dispersal rate ω , total number of local recruits R_{it} , and probability of dispersal between patches p_{ij} :

$$p_{ij} = \frac{e^{-md_{ij}}}{\sum_{\substack{j=1 \\ j \neq i}}^{N_p} e^{-md_{ij}}}$$

where d_{ij} is the pairwise distance between patches, m is the distance cost to dispersal. The summation term in the denominator normalizes the probability of moving to any patch to between 0 and 1 with the constraint that dispersers cannot move back into their home patch (i.e., $j \neq i$). With $\bar{d} = 1$, $m = 0.5$, $\omega = 0.1$, $R_{it} = 100$ in a linear network:

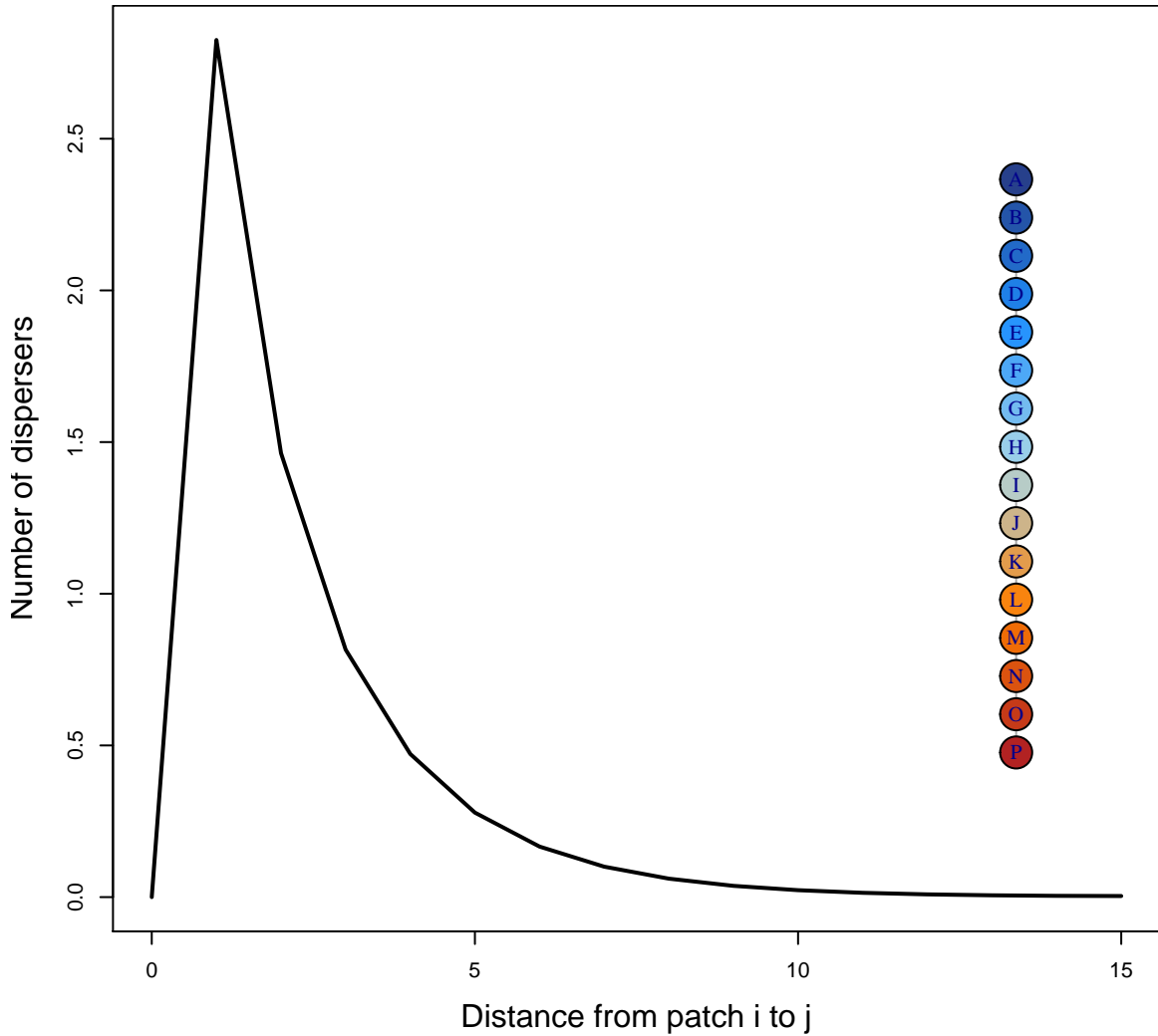


Figure S3: Example dispersal patterns across linear network.

Disturbance regimes

In all scenarios, disturbance was applied after 50 years of equilibrating the metapopulation at pristine conditions. At year 51, we applied the disturbance regime (the regime varied from *uniform*, *localized*, *random*, and *localized, extirpation* - see *Scenarios* below). Disturbance immediately removes a set proportion of the metapopulation adults at that time (i.e., 0.9 of $MN_{t=51}$). Once applied, the metapopulation was no longer disturbed and spatio-temporal recovery dynamics emerged naturally from these new conditions.

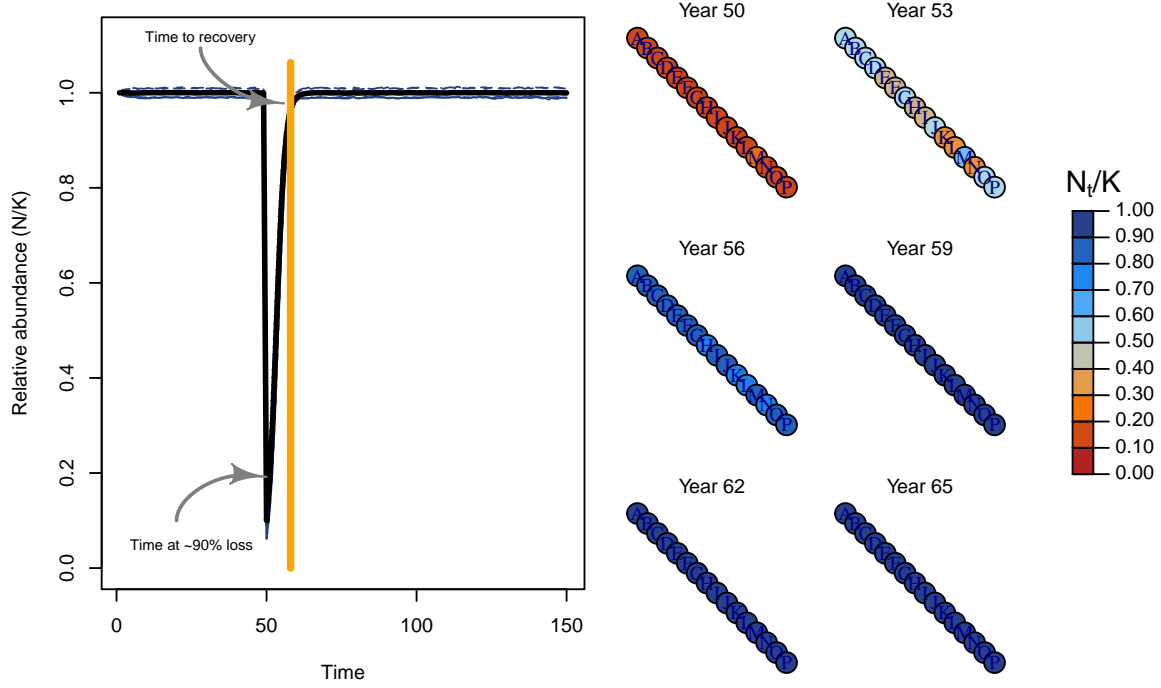


Figure S4: Recovery regime of metapopulation with linear topology through time (left) and space (right).

Recruitment stochasticity

Our model allowed for stochastic recruitment that followed a lognormal distribution with average variation in recruitment of σ_R . In cases of stochastic recruitment, the expected recruitment:

$$R_{it} = \frac{\alpha_i N_{it-1}}{1 + \frac{\alpha_i - 1}{\beta_i} N_{it-1}}$$

becomes:

$$R_{it} = \frac{\alpha_i N_{it-1}}{1 + \frac{\alpha_i - 1}{\beta_i} N_{it-1}} e^{(\epsilon_{it} - \frac{\ln(\sigma_R^2 + 1)}{2})}$$

where lognormal deviates for each patch i at time t are drawn from a multivariate normal distribution (MVN). If σ_R is low, then metapopulation dynamics approach the deterministic case. In some scenarios, we evaluate the role of spatially and/or temporally correlated deviates across the metapopulations to model potential common drivers affecting metapopulation dynamics (e.g., Moran effects). Expected recruitment deviates followed a first-order autoregression model such that:

$$\epsilon_{it} = \rho_T \epsilon_{t-1} + MVN(\mu = 0, \Sigma = \sigma_R(1 - \rho_T^2)e^{(-\rho_S D_{ij})})$$

where ρ_T is temporal correlation (bounded 0 – 1) ρ_S is rate of distance-decay in spatial correlation (bounded 0 – ∞ with higher values leading to independent patches). If ρ_T is 0 and ρ_S is high, then annual recruitment deviates are independent. We illustrate the effects of four kinds of recruitment deviates below using the same random number generator seed:

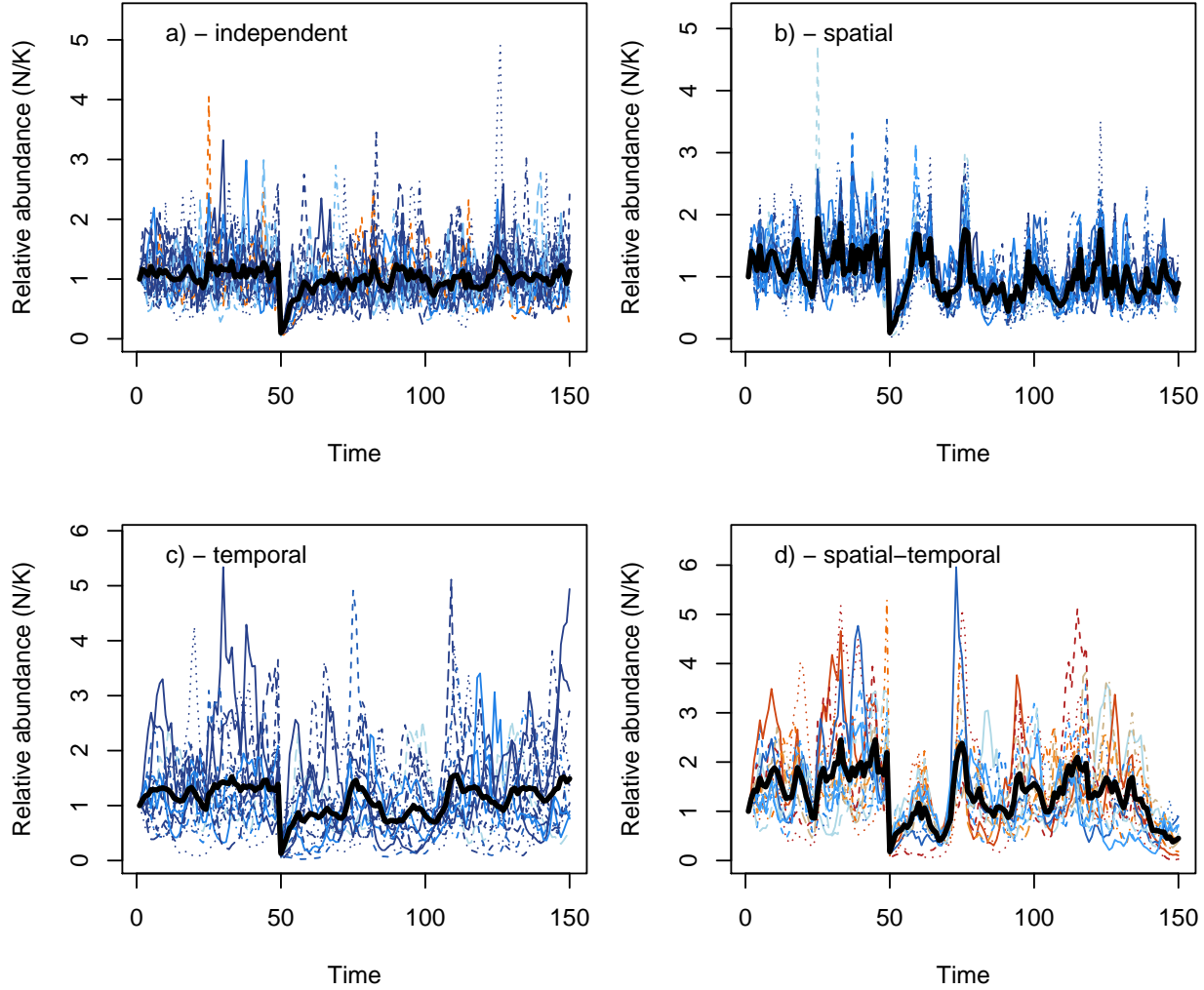


Figure S5: Metapopulation dynamics with independent (a), spatially correlated (b), temporally correlated (c), and spatio-temporally correlated (d) recruitment deviates.

Post-disturbance outcomes

We measured the following post-disturbance outcomes that measure various conservation and recovery processes.

1. Recovered (a) & recovery rate (b) after disturbance - (a) the number of simulations where metapopulation abundance averaged 1.0 of the average pre-disturbance abundance for 5 consecutive years post-disturbance, and (b) the number of years it took to get there.

2. Extinction (a) & extinction rate (b) - (a) the number of simulations where metapopulation abundance was <0.05 carrying capacity, and (b) the mean number of years it took to get there.
3. Patch occupancy - the mean number of patches with >0.1 local carrying capacity.
4. Spatial variance - the variation in patch abundance across patches within a given window of time.
 - a. Within 5 years post-disturbance
 - b. Within 10 years post-disturbance
 - c. Within 25 years post-disturbance
5. Number of populations defined as source, sink, pseudo-sink such that:
 - a. Sources provide surplus recruits and net emigrants such that: $(R_{it} > N_{it}) \& (E_{it} > I_{it})$
 - b. Sinks consume recruits and net immigrants such that: $(R_{it} < N_{it}) \& (E_{it} < I_{it})$
 - c. Pseudo-sinks would provide surplus recruits in the absence of dispersal such that $(R_{it} > N_{it})$ but $(R_{it} + E_{it}) < (R_{it-1} + I_{it-1} - E_{it-1})$
6. Fit stock-recruitment model to aggregate of metapopulation to estimate:
 - a. Recruitment compensation ratio compared to true metapopulation average
 - b. Metapopulation carrying capacities compared to true sum of carrying capacities across metapopulation
 - c. Expected recruitment production to true recruitment production across all patches
 - d. Expected maximum surplus production (we term MSY) to true maximum surplus production across all patches

Monitoring & management at aggregate-scale

While true metapopulation dynamics are controlled by local patch dynamics and dispersal such that:

$$N_{it} = R_{it}\epsilon_{it} + I_{it} - D_{it} - E_{it}$$

$$R_{it} = \frac{\alpha_i N_{it-1}}{1 + \frac{\alpha_i - 1}{\beta_i} N_{it-1}}$$

$$MN_t = \sum_{i=1}^{N_p} N_{it}$$

$$MR_t = \sum_{i=1}^{N_p} R_{it}$$

natural resource managers often monitors and manages at the scale of the metapopulation. Hence, management at this scale inherently defines the stock-recruitment dynamics of the aggregate complex of patches (i.e., metapopulation) as:

$$MR_t = \frac{\hat{\alpha}_t MN_{t-1}}{1 + \frac{\hat{\alpha}_t - 1}{\hat{\beta}_t} MN_{t-1}}$$

where $\hat{\alpha}_t$ is the estimated compensation ratio averaged across the metapopulation at time t and $\hat{\beta}_t$ is the estimated carrying capacity of the entire metapopulation. Necessarily, these estimates emerge from monitoring data collected across all patches and are sensitive to the quality of the data and how local patches perform through time. For example, temporal shifts in productivity regimes may be masked if most of the data were sampled before the regime shift. To help surmount these issues, modern resource assessments use data weighting and penalties (i.e., priors) when fitting models to data.

In our assessment, we weighted recent years of sampling over more distant years such that:

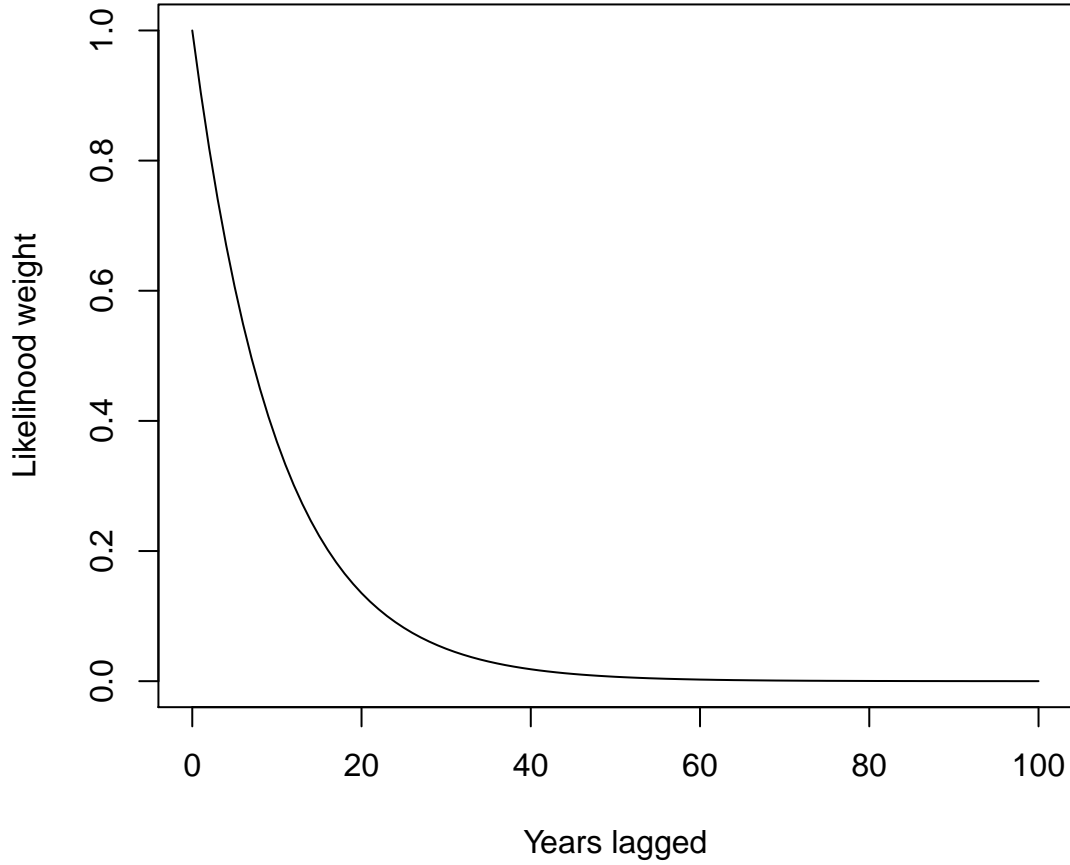


Figure S6: Likelihood weighting for samples collected over time from current year of sampling.

Furthermore, we used penalized normal likelihoods on both $\hat{\alpha}_t$ and $\hat{\beta}_t$ such that:

$$\hat{\alpha}_t \sim N(\mu = \alpha_{t-1}, \sigma = 3\alpha_{t-1})$$

and

$$\hat{\beta}_t \sim N(\mu = \beta_{t-1}, \sigma = 3\beta_{t-1})$$

where $\mu = \alpha_{t-1}$ and $\mu = \beta_{t-1}$ represents the best estimates from the previous assessment and the 3 in the σ term represents a 300% coefficient of variation. We used these penalized likelihoods to fit the above aggregate stock-recruitment model with *lognormal* error to the metapopulation stock-recruit data collected at time t . We used the following function and fitted to the below θ parameters (termed **theta** in the function **optim()** using the L-BFGS-B optimizer with a lower bound on $\hat{\alpha}$ of 1.01 (i.e., constrained to be at least above replacement).

```
SRfn <- function(theta) {
  a.hat <- theta[1]
  b.hat <- exp(theta[2])
  sd.hat <- exp(theta[3])
  rec.mean <- (a.hat * spawnRec$spawners) / (1 + ((a.hat - 1) / b.hat) * spawnRec$spawners)
```



```

# negative log likelihood on recruitment parameters
nll <- -1 * sum(dlnorm(spawnRec$recruits, meanlog = log(rec.mean), sdlog = sd.hat,
  log = TRUE) * spawnRec$weights, na.rm = TRUE)
# penalized likelihood on estimated alpha
penalty1 <- -dnorm(a.hat, alphaLstYr, 3 * alphaLstYr, log = TRUE)
# penalized likelihood on estimated carrying capacity
penalty2 <- -dnorm(b.hat, metaKLstYr, 3 * metaKLstYr, log = TRUE)
jnll <- sum(c(nll, penalty1, penalty2), na.rm = TRUE)
return(jnll)
}

```

149 This above function allows us to assess the bias in $\hat{\alpha}_t$, $\hat{\beta}_t$, and $\hat{M}R_t$ compared to true $\bar{\alpha}$, $\bar{\beta}$, and MR_t across
150 the metapopulation. This then allows us to see how much information management & monitoring programs
151 are missing when they assess metapopulations at the aggregate (rather than local) scales.

152 Finding maximum sustainable yield

153 Resource managers measure productivity with a variety of performance reference points. One of the most
154 widely used metrics, commonly called *Maximum Sustainable Yield* in fisheries and other harvest literature
155 (*MSY*), relates to the largest loss the population can sustain over an indefinite period of time while maximizing
156 its ability to replenish itself. Under density-dependent growth, individuals' growth, survival, and reproduction
157 at low population densities are not constrained by limited resources, but overall production is low because
158 there are few individuals. At high densities, limited resources increasingly constrain individual's reproductive
159 success until the population reaches carrying capacity, and overall production drops to zero because per-capita
160 success is low. However, at some intermediate densities, both per-capita and overall production is high, and
161 population growth is at its maximum point due to the large number of reproducing individuals. At this
162 point, there is the maximum surplus of individuals produced above replacement that can help to withstand
163 disturbance or harvest regimes and contribute to future recovery, either through increasing local patch
164 densities or by emigrating neighboring patches providing "rescue effects".

165 Under Beverton-Holt or Ricker density-dependent recruitment, however, there exists no analytical solution for
166 calculating *MSY*. Therefore, we used numerical methods and a one dimensional root finder to iteratively
167 search for the population mortality that maximized surplus production in the metapopulation. We term this
168 mortality F_{MSY} and can use this mortality value to calculate maximum surplus production *MSY*, the adult
169 densities that produce *MSY* (termed N_{MSY}), and the recruits that result from this (termed R_{MSY}).

```

# uniroot numerical search

yieldRoot <- function(alpha, beta, Fcur, model) {
  Ucur <- 1 - exp(-Fcur)
  if (model == "Beverton-Holt") {
    # population model is  $R \sim (CR * S) / (1 + (CR - 1) / K * S)$ : reparameterized
    # Beverton-Holt
    adults <- beta * exp(-Fcur)
    recruits <- (alpha * adults) / (1 + ((alpha - 1) / beta) * adults)
    yield <- recruits - adults
  }
  if (model == "Ricker") {
    # population model is  $R \sim CR * S * e^{(-\log(CR) / K * S)}$ : reparameterized Ricker
    adults <- beta * exp(-Fcur)
    recruits <- alpha * adults * exp((-log(alpha) / beta) * adults)
    yield <- recruits - adults
  }
  return(list(recruits = recruits, adults = adults, yield = yield))
}

```

```

}

# Return approximate gradient for integral

fun_yield <- function(Fcur, alpha, beta, delta, model) {
  y1 <- yieldRoot(alpha = alpha, beta = beta, Fcur = Fcur - delta/2, model = model)$yield
  y2 <- yieldRoot(alpha = alpha, beta = beta, Fcur = Fcur + delta/2, model = model)$yield
  approx.gradient <- (y2 - y1)/delta
  return(approx.gradient)
}

# uniroot search for optimal yield and Fmsy
findMSY <- function(alpha, beta, Npatches, model) {
  F_msy <- NULL
  for (i in 1:Npatches) {
    a_p <- alpha[i]
    b_p <- beta[i]
    F_msy[i] <- uniroot(fun_yield, interval = c(0, 1), extendInt = "yes",
      alpha = a_p, beta = b_p, delta = 1e-04, model = model)$root
  }
  MSY <- sapply(1:Npatches, function(x) {
    yieldRoot(alpha = alpha[x], beta = beta[x], Fcur = F_msy[[x]][1], model = model)
  })
  return(list(F_msy = F_msy, MSY = MSY))
}

```

Scenarios

We tested all combinations of the following eight processes (below) and ran a 100 bootstraps per scenario to estimate the mean for each of the above outcomes.

1. Homogenous and spatially variable recruitment compensation ratio across patches, i.e. intrinsic rate of population growth (α_i).
2. Homogenous and spatially variable local carrying capacity across patches, i.e. asymptote of expected recruits at high adult densities (β_i).
3. Disturbances where a proportion of individuals removed from metapopulation (e.g., 0.90) occurs.
 - a. *uniform* - random individuals removed at equal vulnerability across all patches.
 - b. *localized, random* - random individuals removed from randomly selected subset of patches (as long as the target individuals lost in the metapopulation can be achieved in that subset of patches)
 - c. *localized, extirpation* - total extirpation of randomly selected subset of patches (as long as the target individuals lost in the metapopulation can be achieved in that subset of patches)
4. Density-independent dispersal rates ω from 0 to 20% of individuals within a patch will disperse.
5. Topology of the spatial networks with linear, dendritic, star, and complex networks. Each network with N_p of 16 and distance between patches \bar{d} of 1.
6. Stochastic recruitment deviates from low, medium, high coefficient of variation on lognormal error. Generate stochasticity in time-dynamics via random recruitment deviates away from expected.
7. Temporal correlation in recruitment deviates from low, medium, high correlation (i.e., good year at time t begets good year at time $t+1$).

8. Spatial correlation in recruitment deviates among patches from low, medium, to high correlation (i.e., neighboring patches go up or down together).

Example results

We demonstrate our metapopulation model with an example outcome for a linear network composed of 16 patches, a dispersal rate of 0.01 and a high enough dispersal cost such that individuals are only willing to move to their closest neighboring patches. This limits the strength of potential rescue effects. For this example, patches varied in their productivity and carrying capacity but will have deterministic population dynamics.

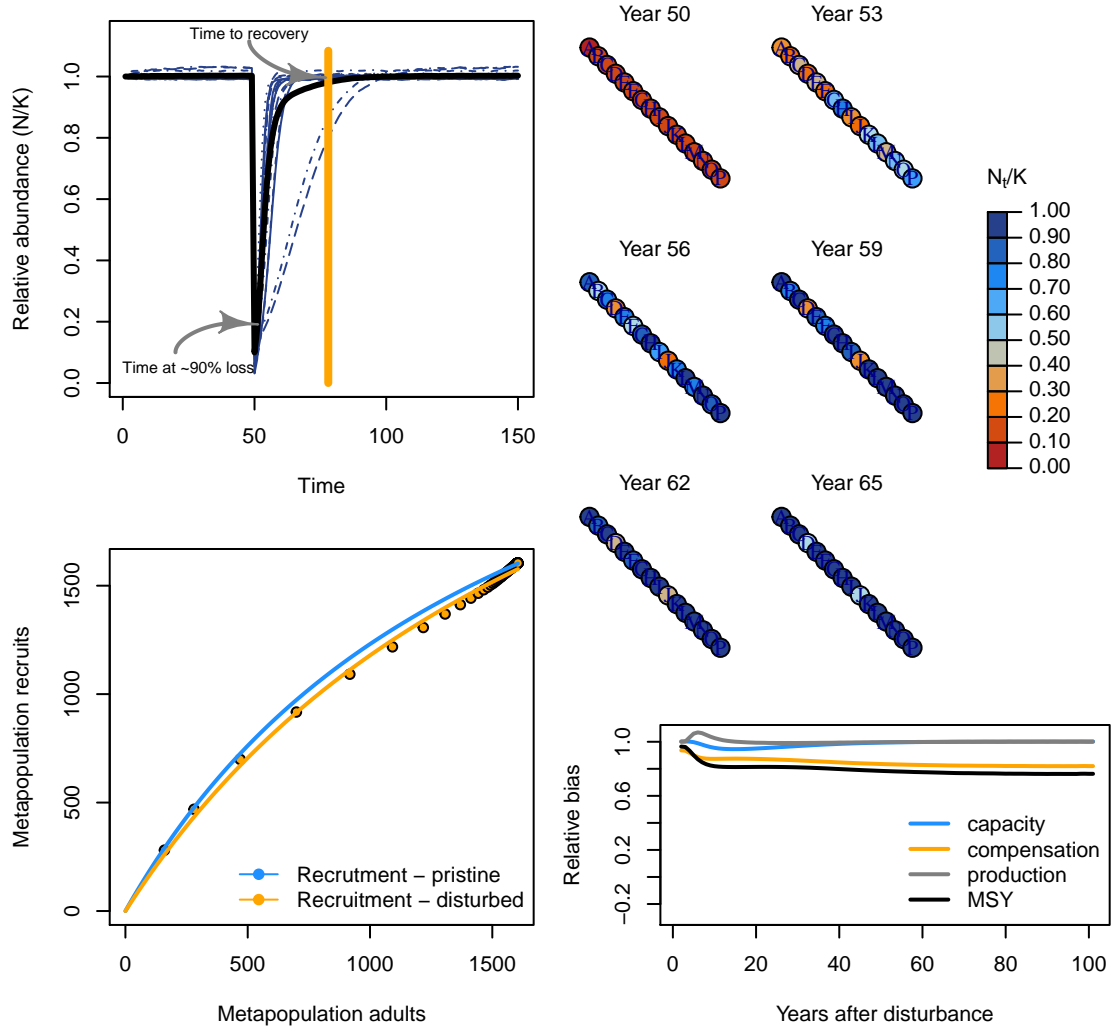


Figure S7: Spatial recovery regime of metapopulation with linear topology through time (top left) and space (top right). Recruitment dynamics before and 10 years after disturbance (bottom left). Relative bias in aggregate-scale estimates of carrying capacity, compensation ratio, and recruitment production in recovery phase (bottom right).

We can then contrast this with a different network shape, like a dendritic network.

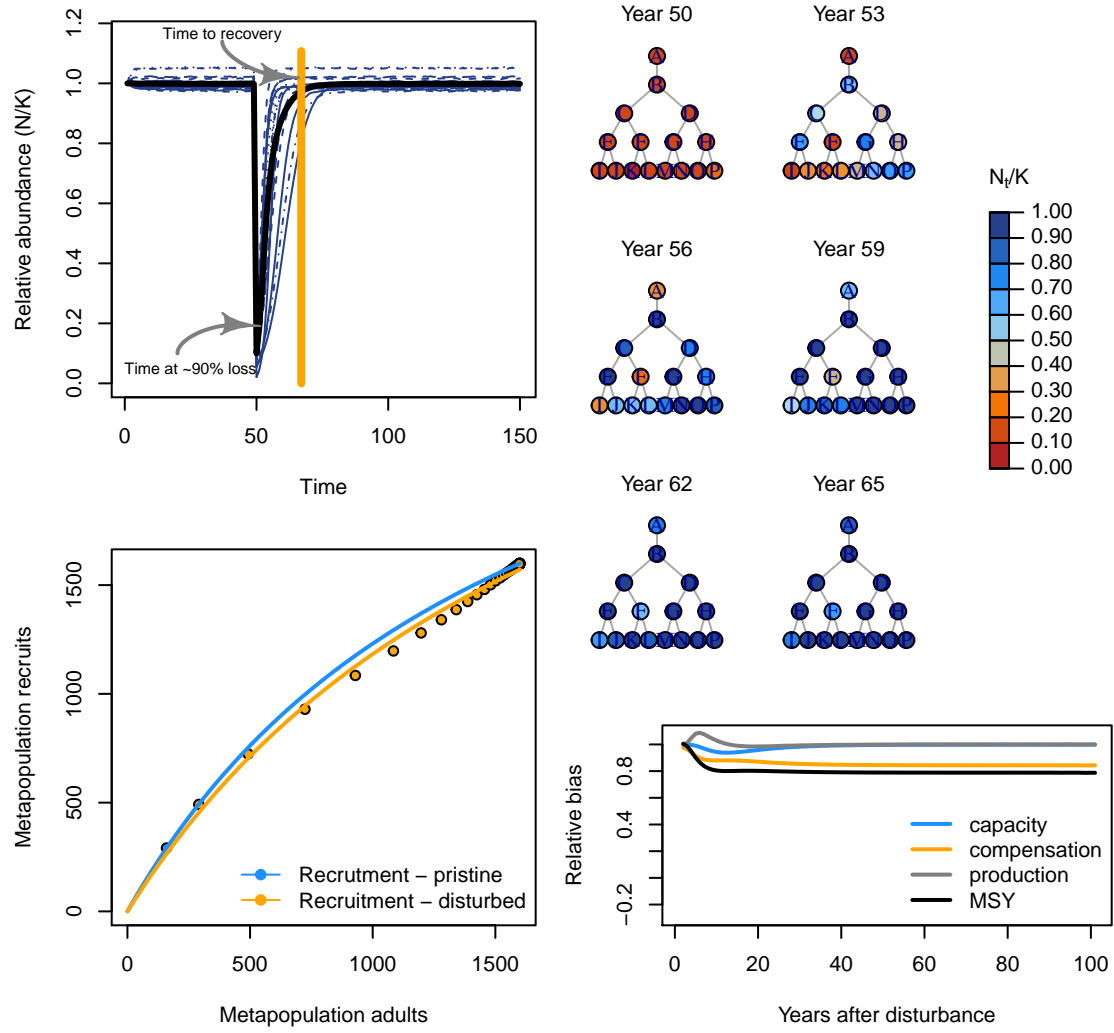


Figure S8: Spatial recovery regime of metapopulation with dendritic topology.

199 Now, let's add some stochasticity to recruitment and see how this affects the recovery regime.

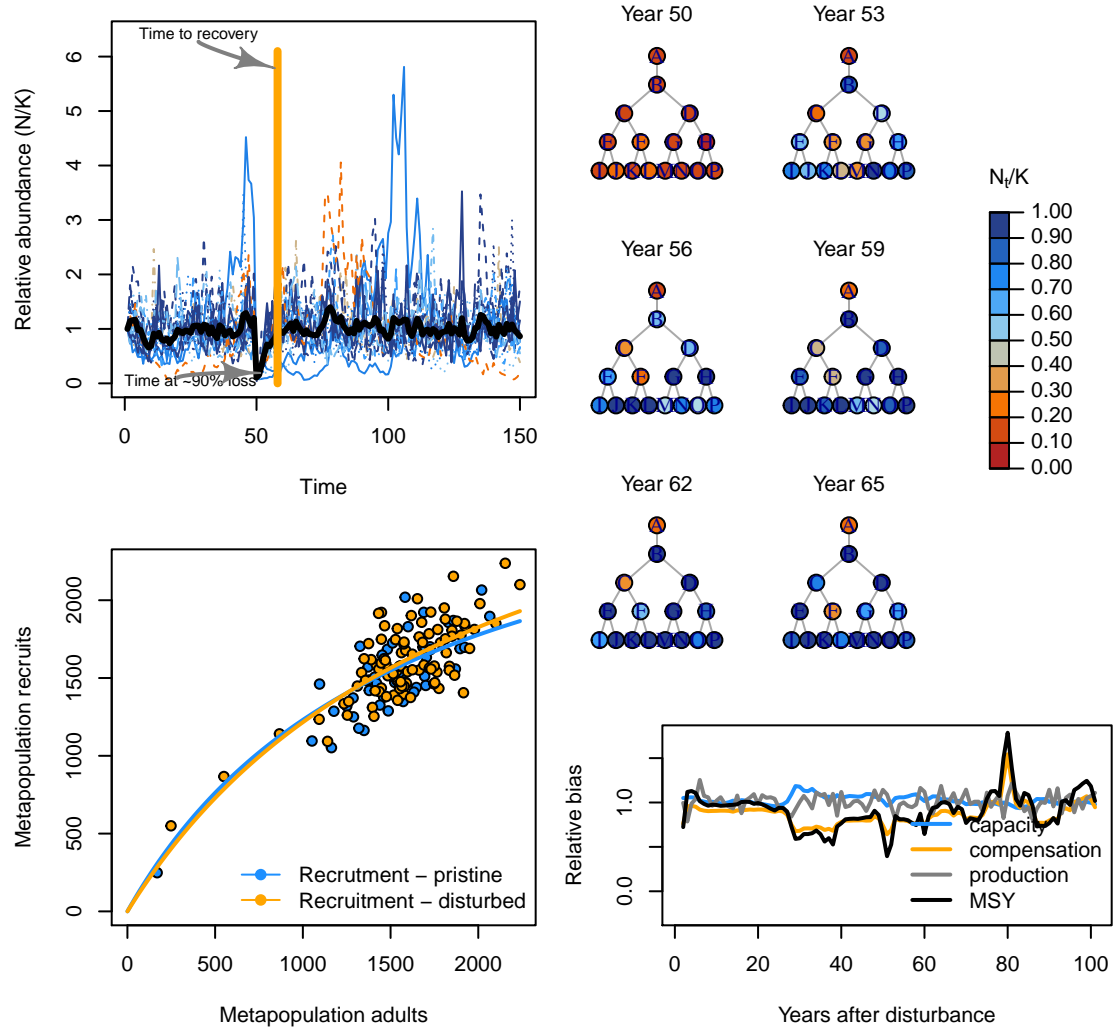


Figure S9: Spatial recovery regime of stochastic metapopulation.

Next, we can contrast with a disturbance regime where the disturbance is concentrated on local patches that can be completely extirpated (rather than the disturbance being applied proportionally across all patches e.g., a mixed-stock fishery).

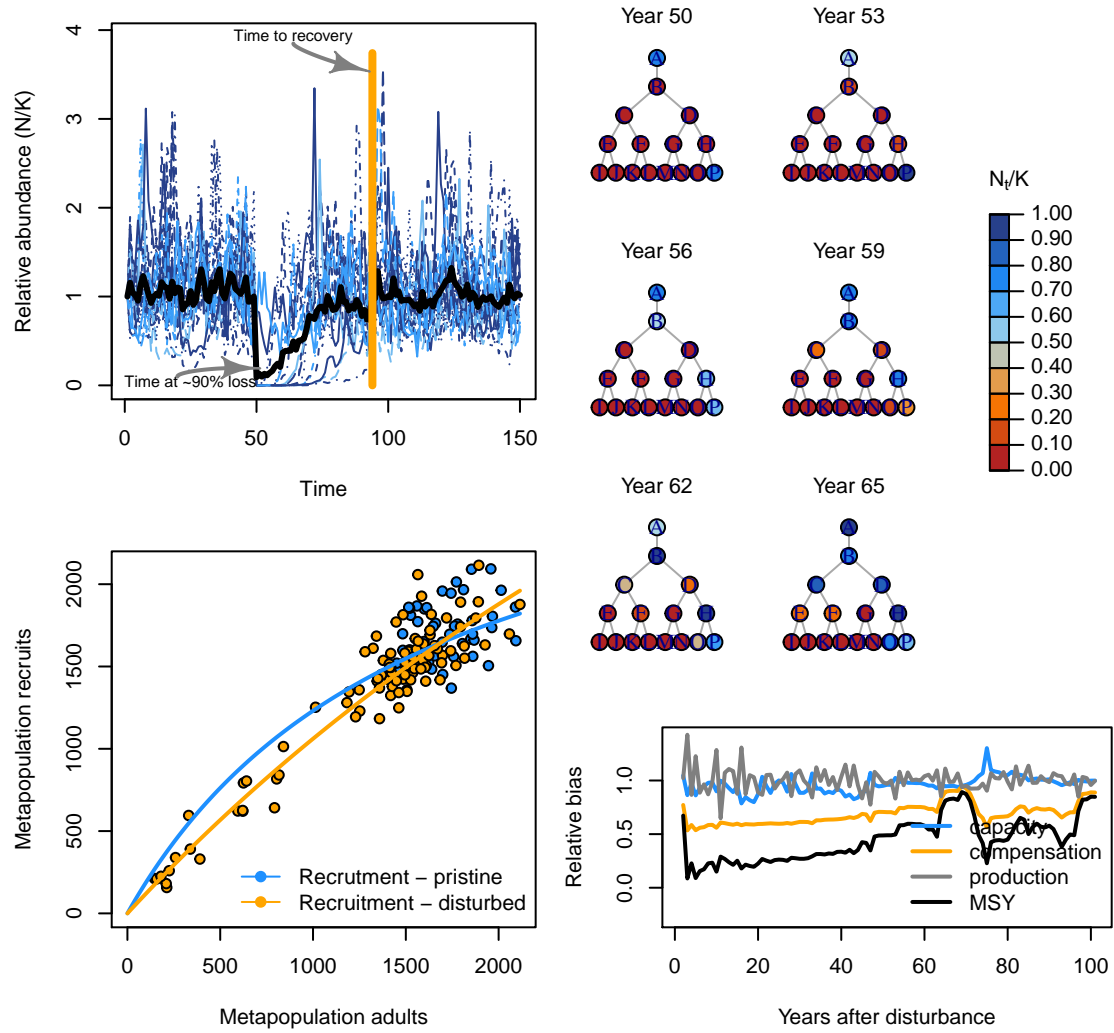


Figure S10: Spatial recovery regime of stochastic metapopulation.

Simulation test & bootstrap

General patterns

Effects of disturbance regime

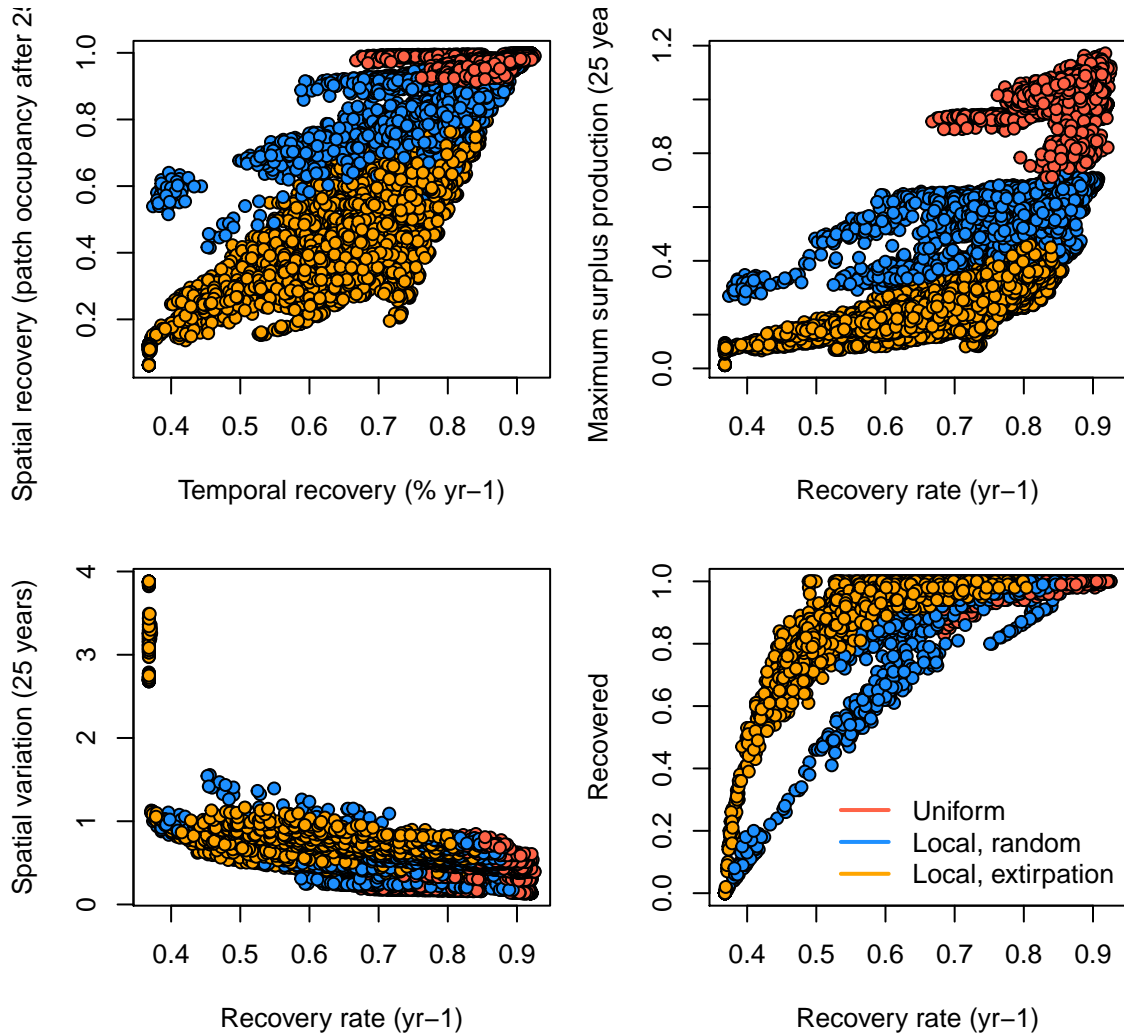


Figure S11: Spatial and temporal recovery patterns along disturbance regimes.

We now show some general patterns in how variable patch demographic rates, network structure, dispersal, disturbance, recruitment stochasticity, and spatio-temporal correlations variation affects metapopulation recovery rates, maximum sustainable yield (i.e., analogous to the maximum rate of loss the system can sustain), and coefficient of variation across patches.

First, let's show recovery rates for a scenario where (1) patches have the same local productivities and carrying capacities, (2) patches have different productivities and carrying capacities, (3) recruitment is deterministic and patches are different, and (4) spatial-temporal correlation in stochastic recruitment.

Below, we can see three main effects on recovery rates (number of generations to reach recovery). First, recovery gets faster with increased dispersal. Most of the action here takes place at low rates of dispersal indicating most spatial topologies don't need much dispersal to quicken their recovery. In preliminary runs, dispersal rates of 0.05–0.2 provided similar recovery patterns. Second, more localized disturbances regimes lead to slower recovery. Third, linearized networks have slower recovery times than interconnected, complex networks suggesting that rescue effects take some time to cascade through the entire network of patches.

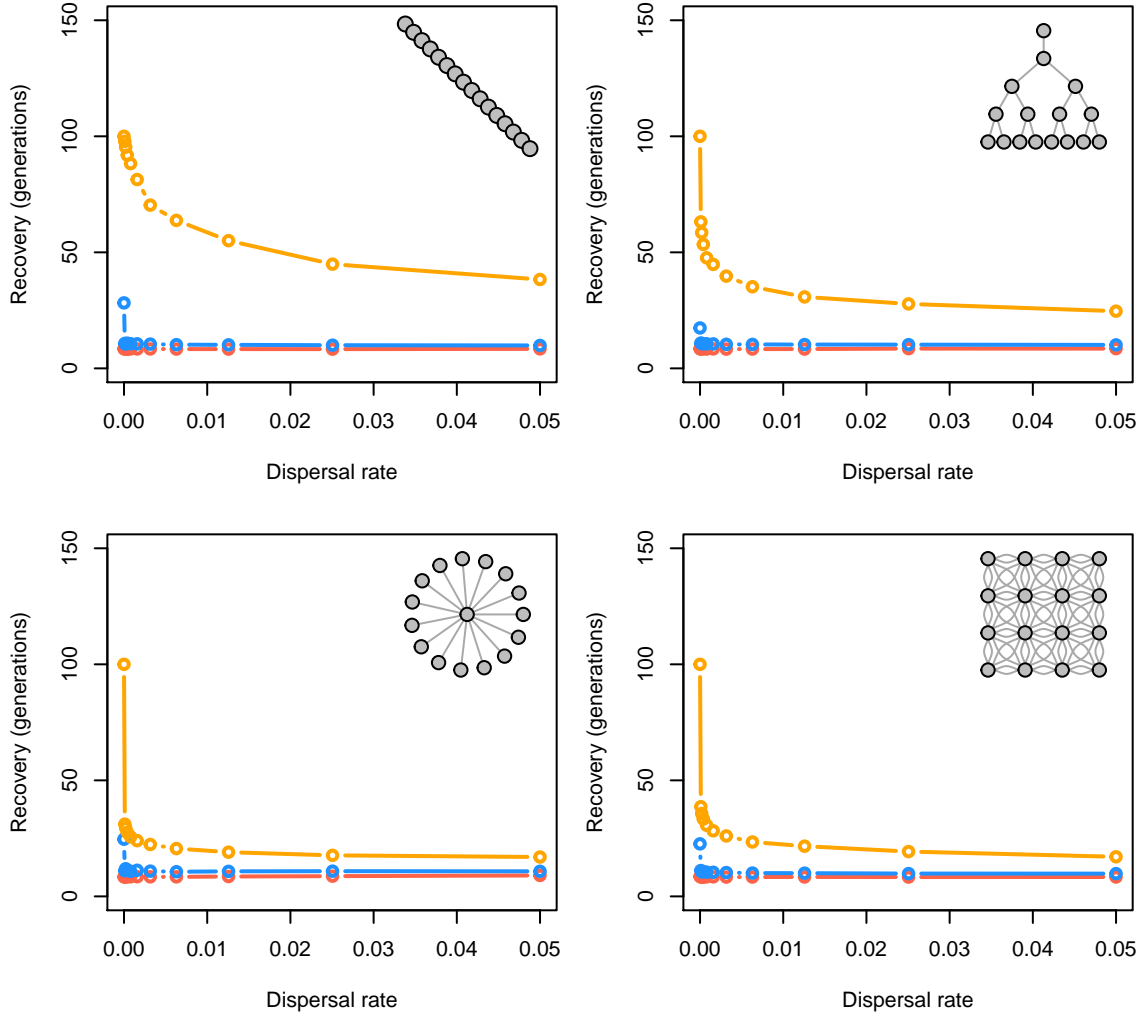


Figure S12: Recovery rates along dispersal, disturbance (red - uniform; blue - localized, random; orange - localized, extirpation), and network gradients without stochasticity.

219 Now, lets show recovery rates for the same scenario with deterministic recruitment but allowing for patches to
 220 vary in productivity and carrying capacity. In addition to the same three main effects of dispersal, network,
 221 and disturbance noted above, we also see variable patch productivities slows recovery across all scenarios.

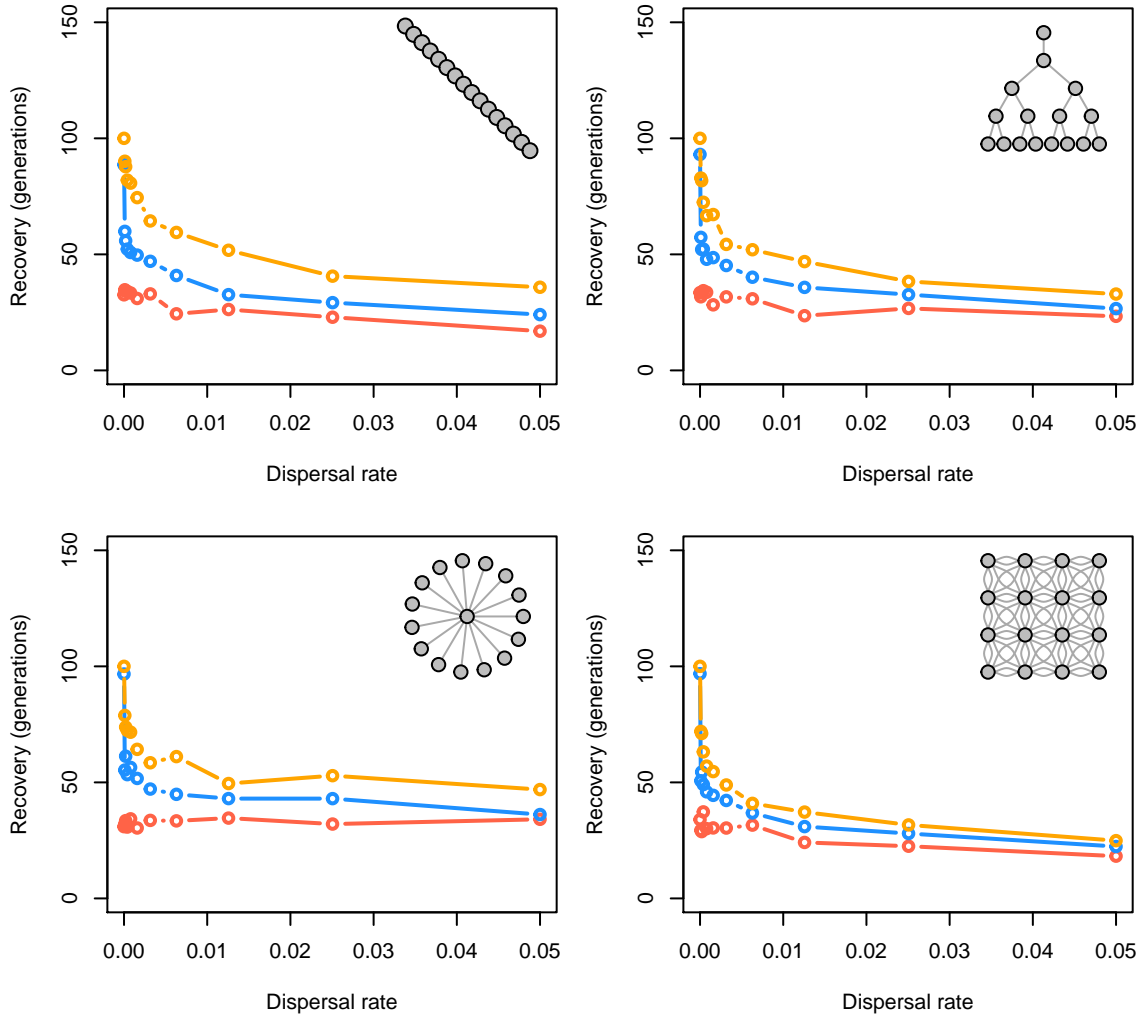


Figure S13: Recovery rates along dispersal, disturbance (red - uniform; blue - localized, random; orange - localized, extirpation), and network gradients with variable local productivity and carrying capacities.

Now, let's show recovery rates for the same scenario but allowing for recruitment to be stochastic (but patches are the same in demography). We see the same three main effects of dispersal, network, and disturbance noted above. We also see a few subtle changes: (1) stochasticity slows recovery for uniform and local disturbance, but (2) quickens recovery for extreme local disturbance.

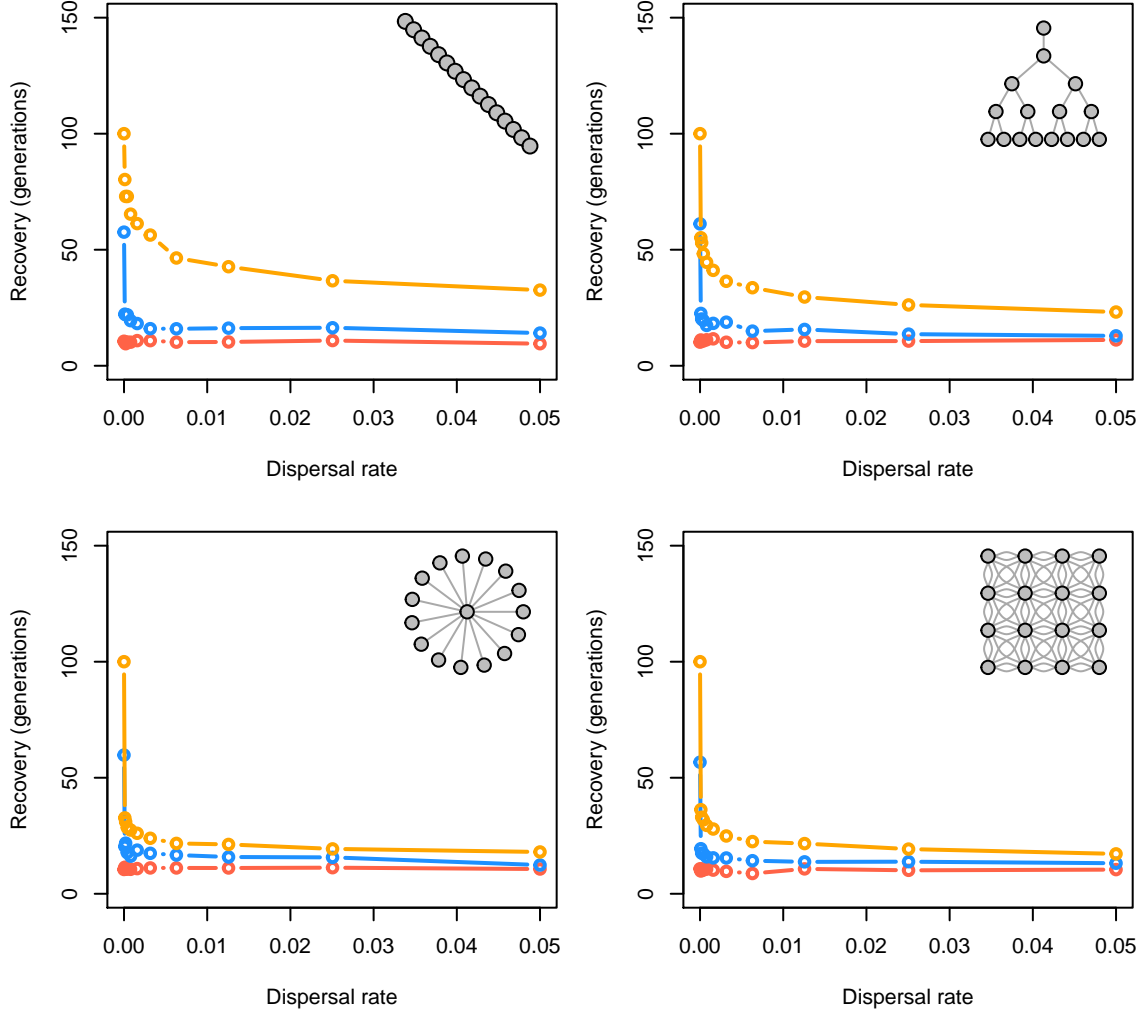


Figure S14: Recovery rates along dispersal, disturbance (red - uniform; blue - localized, random; orange - localized, extirpation), and network gradients with stochasticity.

Now, let's show recovery rates for the same scenarios but with spatial and temporal correlations in recruitment stochasticity. In addition to the same effects of stochasticity, we also generally see a small effect of slower recovery times for uniform and local disturbance, but faster recovery times for extreme localized disturbance.

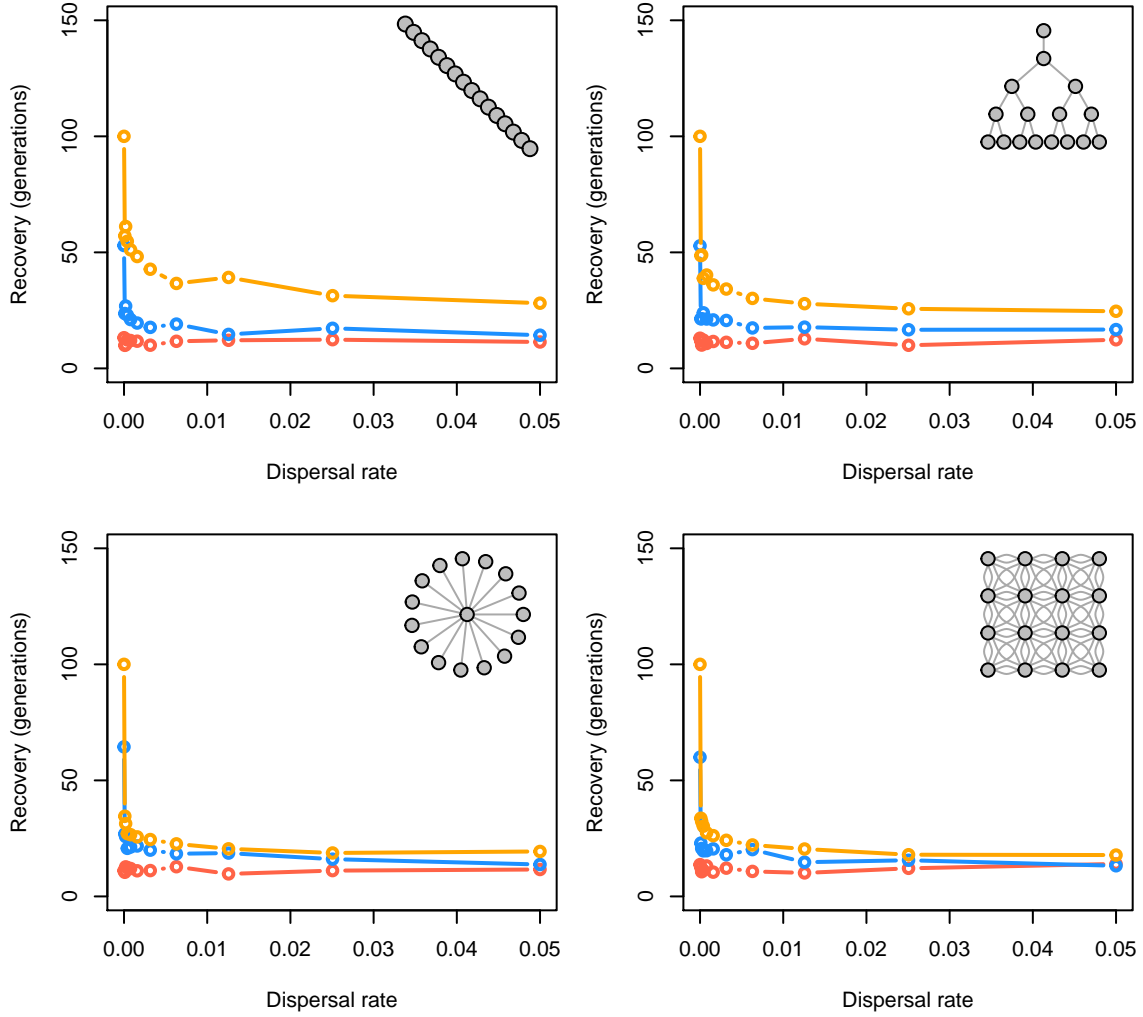


Figure S15: Recovery rates along dispersal, disturbance (red - uniform; blue - localized, random; orange - localized, extirpation), and network gradients with high spatial-temporal correlation in recruitment variation.

General patterns in MSY

MSY with deterministic recruitment where patches are the same

We now show similar patterns in how the maximum surplus production of the whole metapopulation (i.e., MSY) shifts in the first 10 years post-disturbance compared to the sum of MSY for each patch. A value of 1.0 would indicate that the disturbed metapopulation can sustain itself against the same disturbance regime as the sum of each patch independently. In other words, is the metapopulation more, less, or equal to the sum of its parts.

We will show 10-year MSY patterns for a scenario where (1) patches have the same local productivities and carrying capacities, (2) patches have different productivities and carrying capacities, (3) recruitment is deterministic and patches are different, (4) spatial-temporal correlation in stochastic recruitment.

Below, we can see three main effects on recovery rates (number of generations to reach recovery). First, recovery gets faster with increased dispersal. Most of the action here takes place at low rates of dispersal indicating most spatial topologies don't need much dispersal to quicken their recovery. In preliminary runs, dispersal rates of 0.05–0.2 provided similar recovery patterns. Second, more localized disturbances regimes lead to slower recovery. Third, linearized networks have slower recovery times than interconnected, complex networks suggesting that rescue effects take some time to cascade through the entire network of patches.

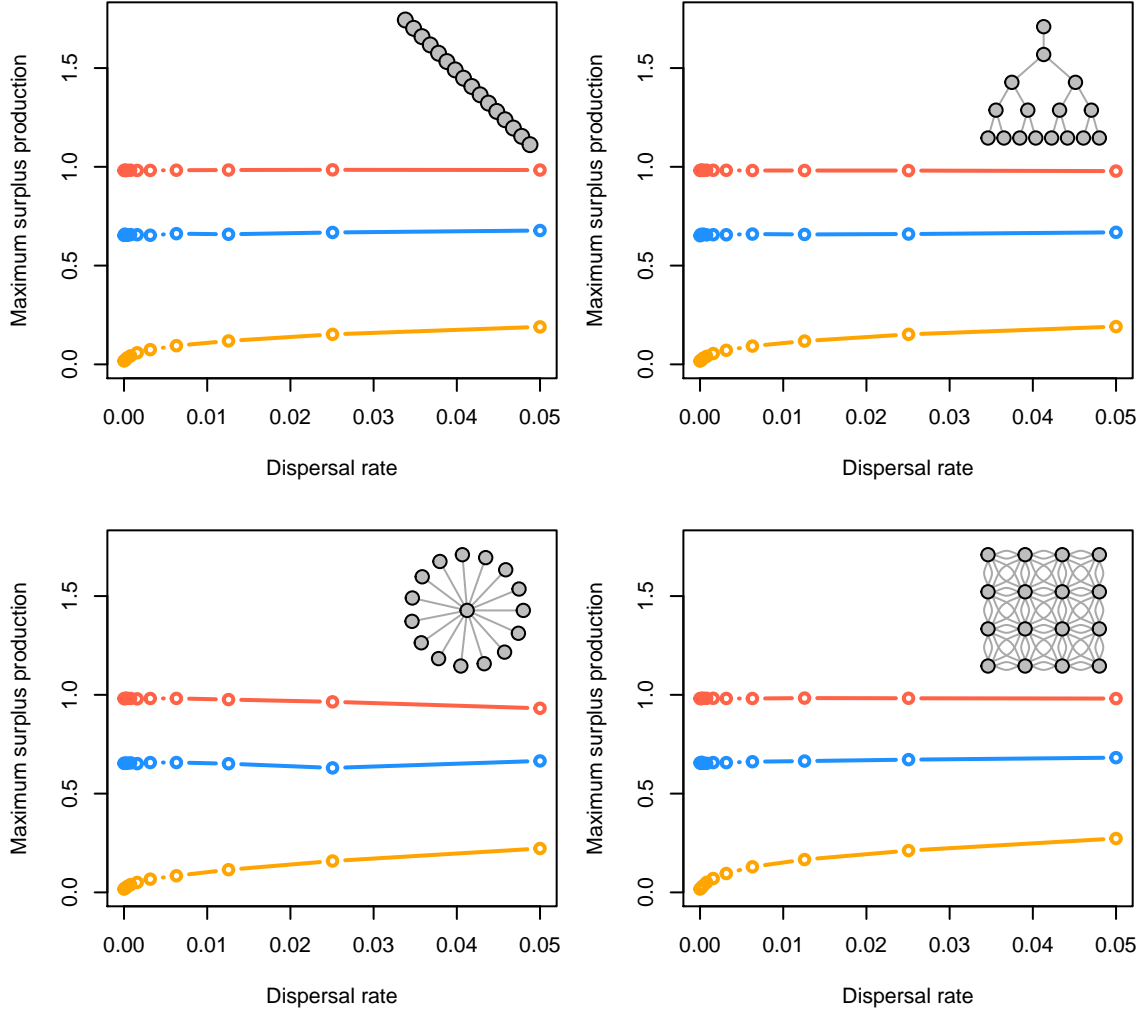


Figure S16: Maximum surplus production along dispersal, disturbance (red - uniform; blue - localized, random; orange - localized, extirpation), and network gradients with deterministic recruitment and the same patches.

245 **MSY with variable patches**

246 Now, we illustrate how variable patch demography affects the 10-year average MSY.

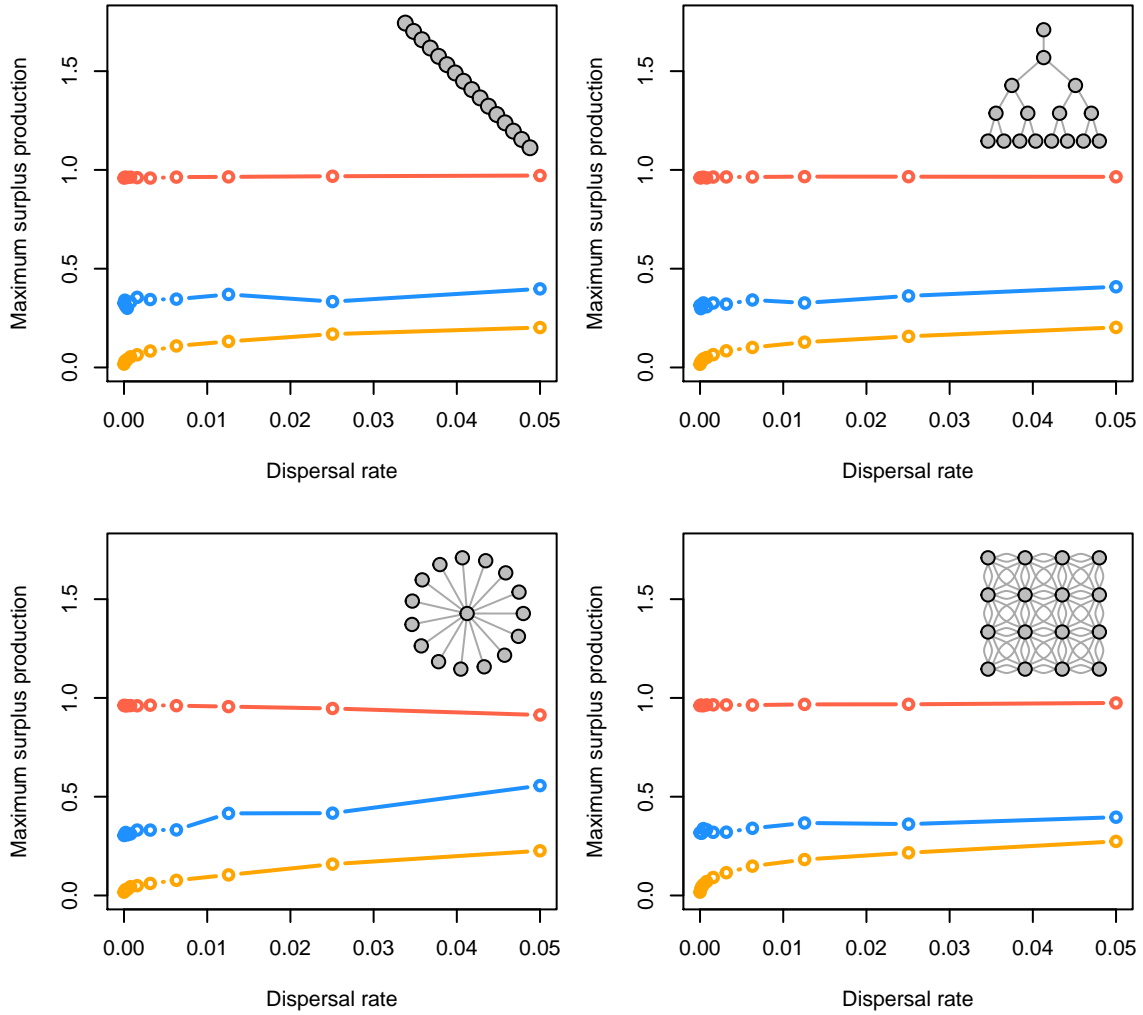


Figure S17: Maximum surplus production along dispersal, disturbance (red - uniform; blue - localized, random; orange - localized, extirpation), and network gradients with variable patches.

247 **MSY with variable patches and stochasticity**

248 Now, we illustrate how variable patch demography affects the 10-year average MSY.

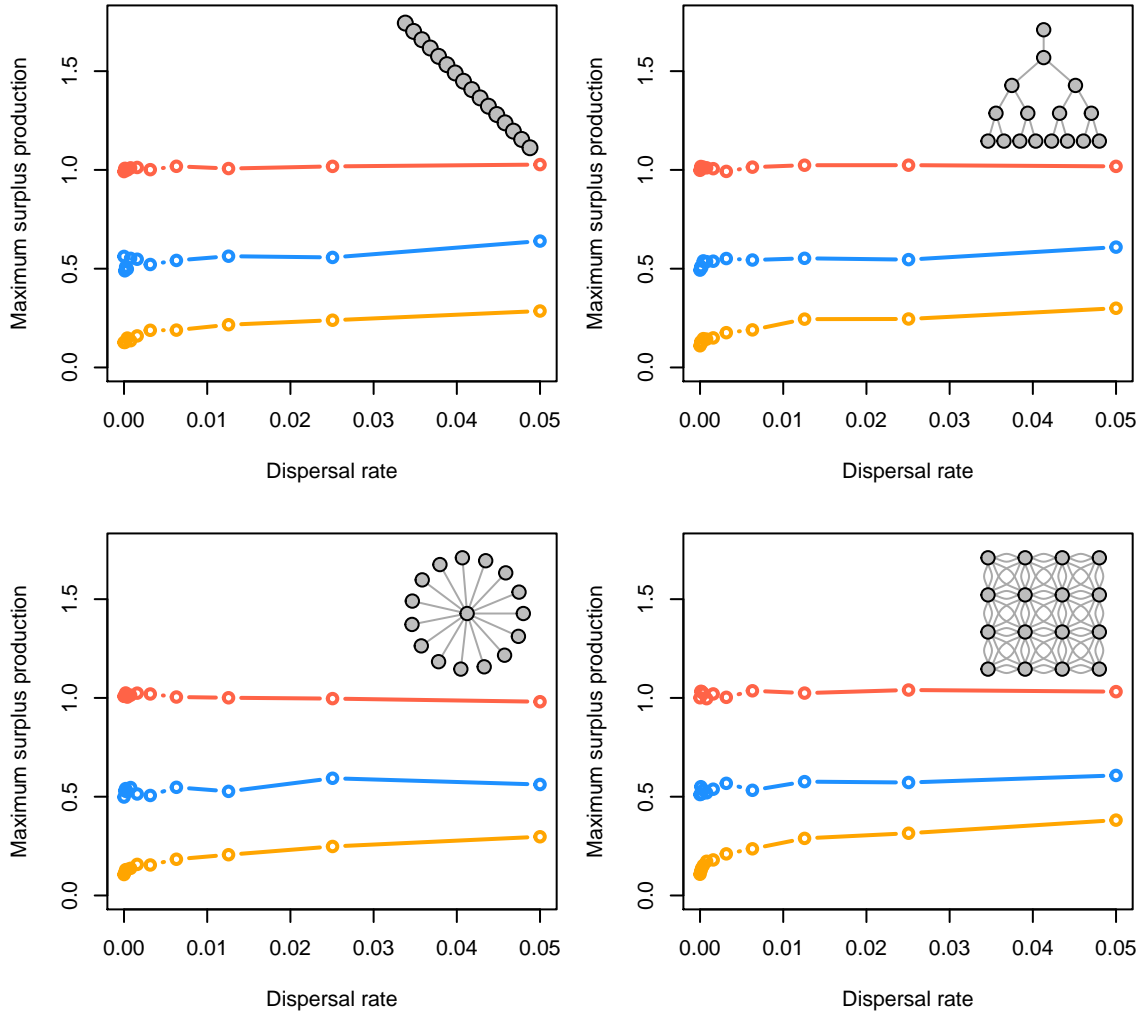


Figure S18: Maximum surplus production along dispersal, disturbance (red - uniform; blue - localized, random; orange - localized, extirpation), and network gradients with variable patches and stochasticity.

249 **MSY with variable patches, and spatio-temporally correlated stochasticity**

250 Now, we illustrate how variable patch demography and high spatial-temporal correlations in stochastic
 251 recruitment affects the 10-year average MSY.

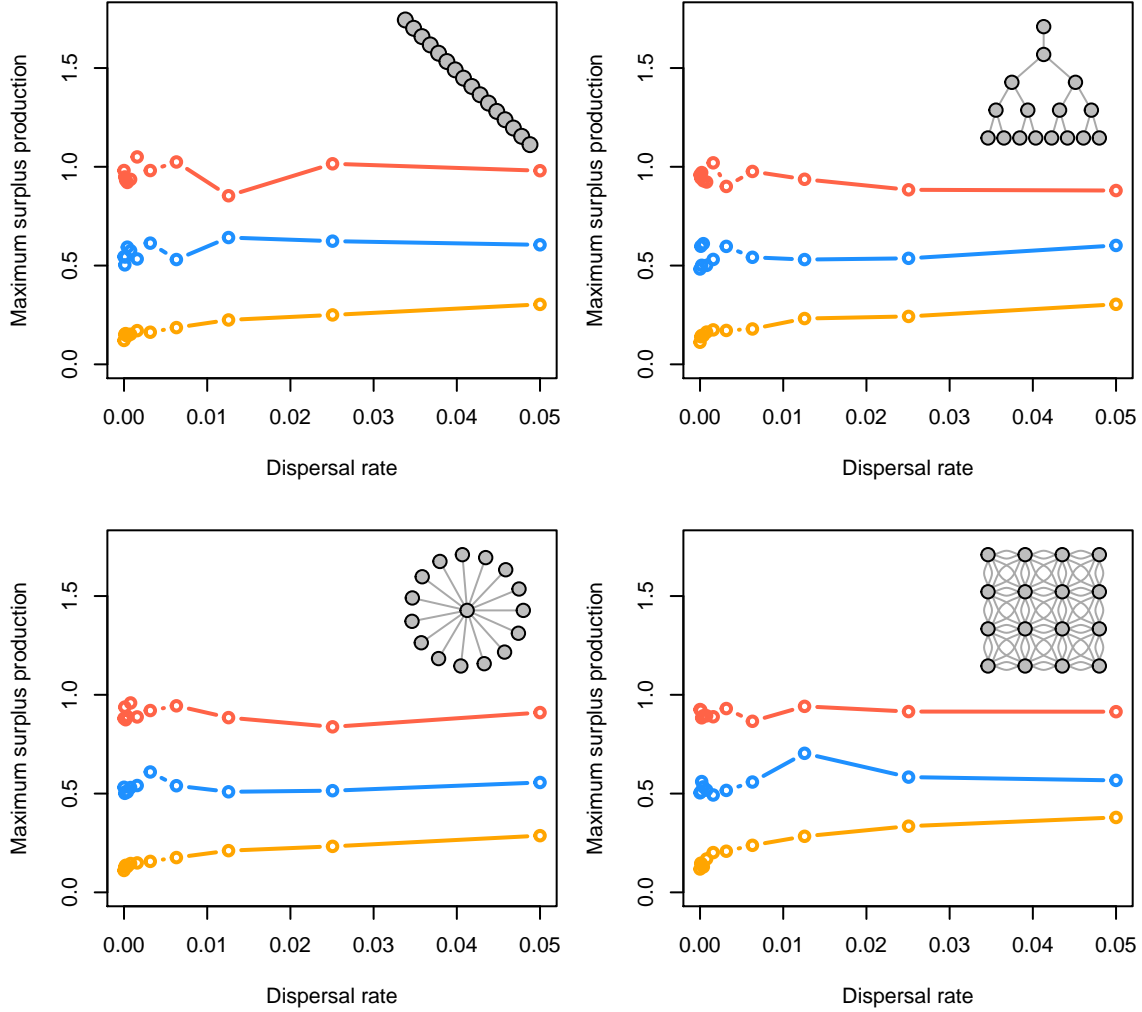


Figure S19: Maximum surplus production along dispersal, disturbance (red - uniform; blue - localized, random; orange - localized, extirpation), and network gradients with high spatial-temporal correlation in recruitment stochasticity and variable patches.

General patterns in the risk of hysteresis & state shifts

Proportion of simulations where the metapopulation either failed to recover or experienced spatial contraction for scenario with deterministic recruitment where patches are the same

We now show similar patterns in the lack of recovery across the metapopulation after 100 generations post-disturbance.

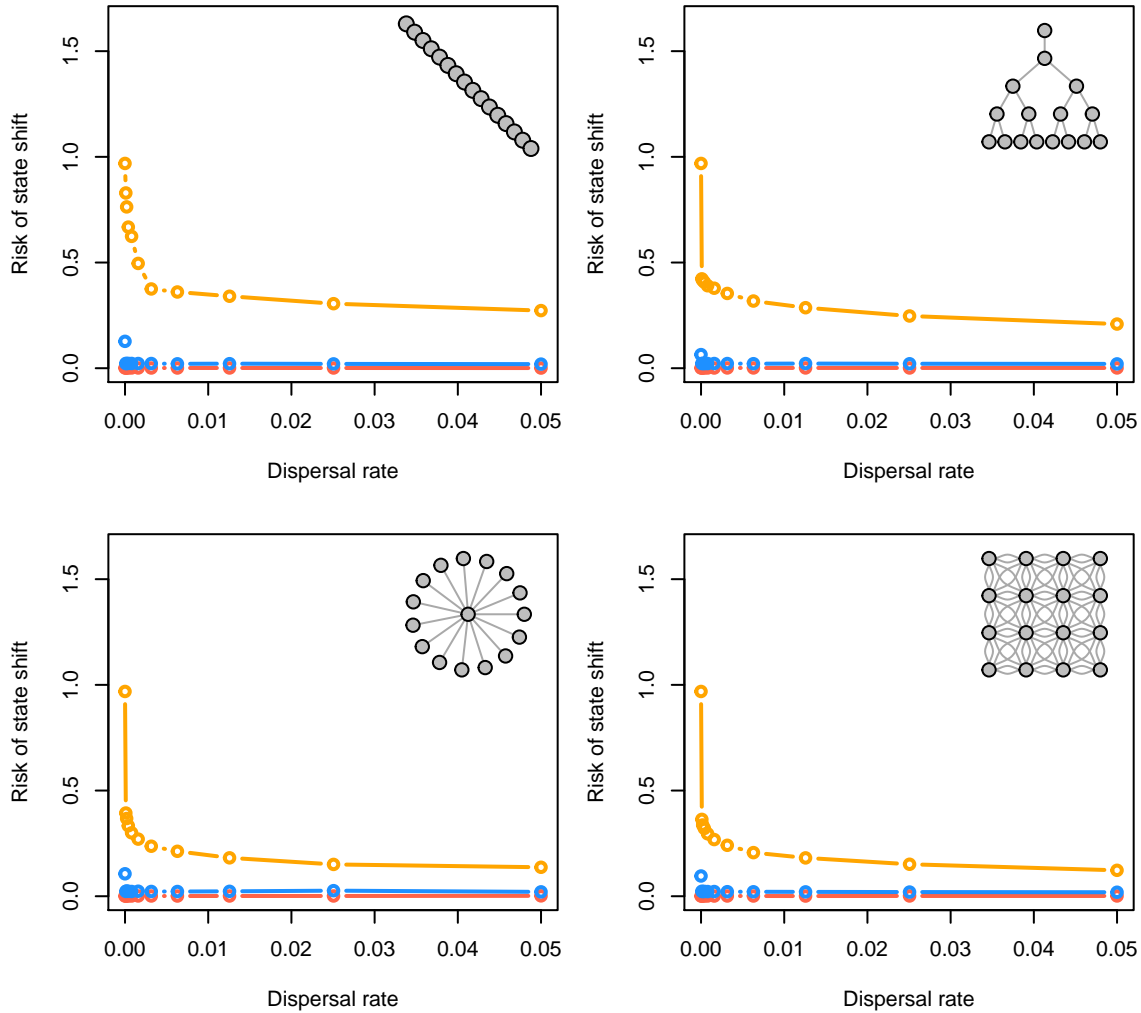


Figure S20: Risk of state shift after 100 generations along dispersal, disturbance (red - uniform; blue - localized, random; orange - localized, extirpation), and network gradients with high spatial-temporal correlation in recruitment variation.

Lack of recovery with variable patches

Now, we illustrate how variable patch demography affects the risk of a state shift.

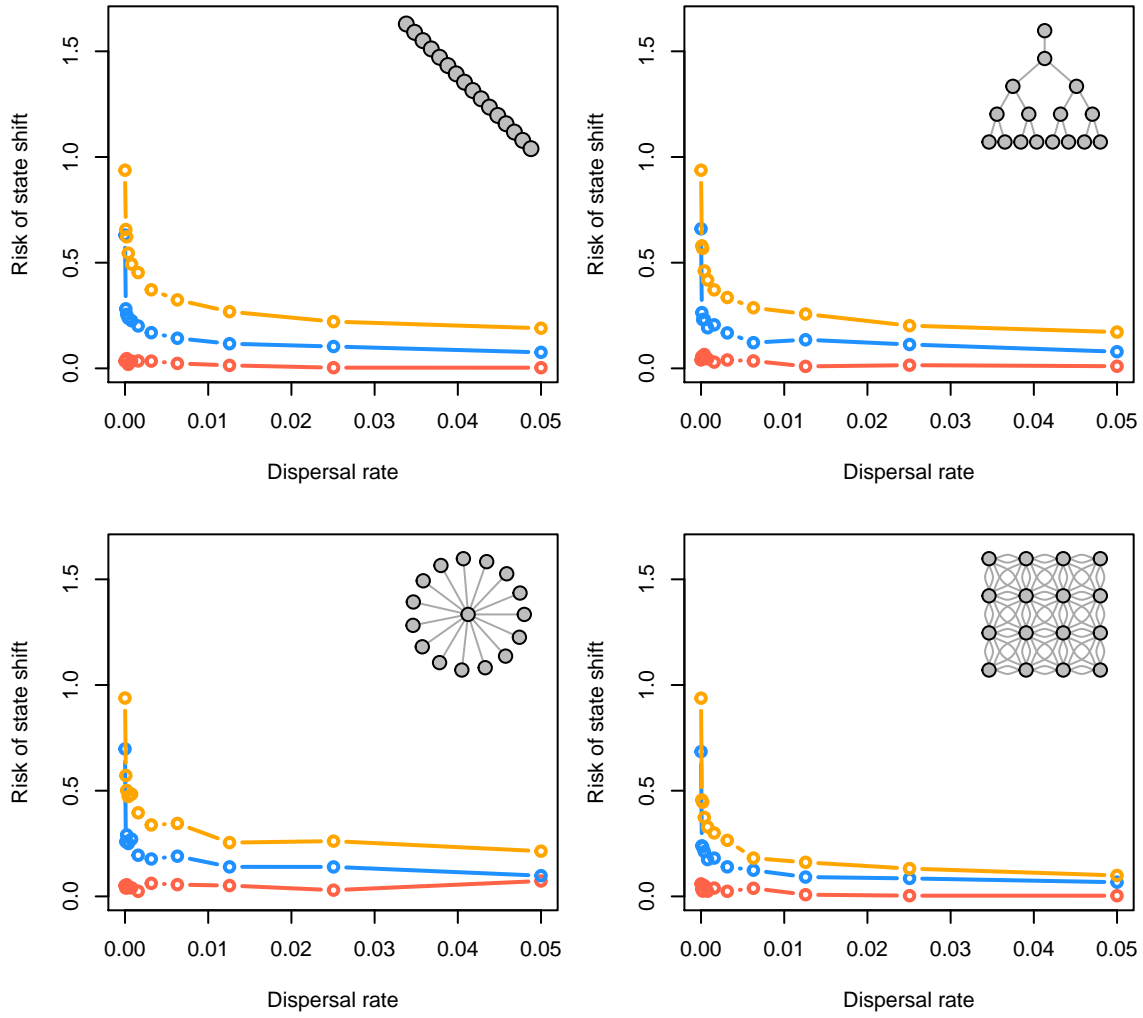


Figure S21: Risk of state shift after 100 generations along dispersal, disturbance (red - uniform; blue - localized, random; orange - localized, extirpation), and network gradients with variable patches.

State shifts with variable patches and stochasticity

Now, we illustrate how variable patch demography and stochastic recruitment affects the risk of state shift.

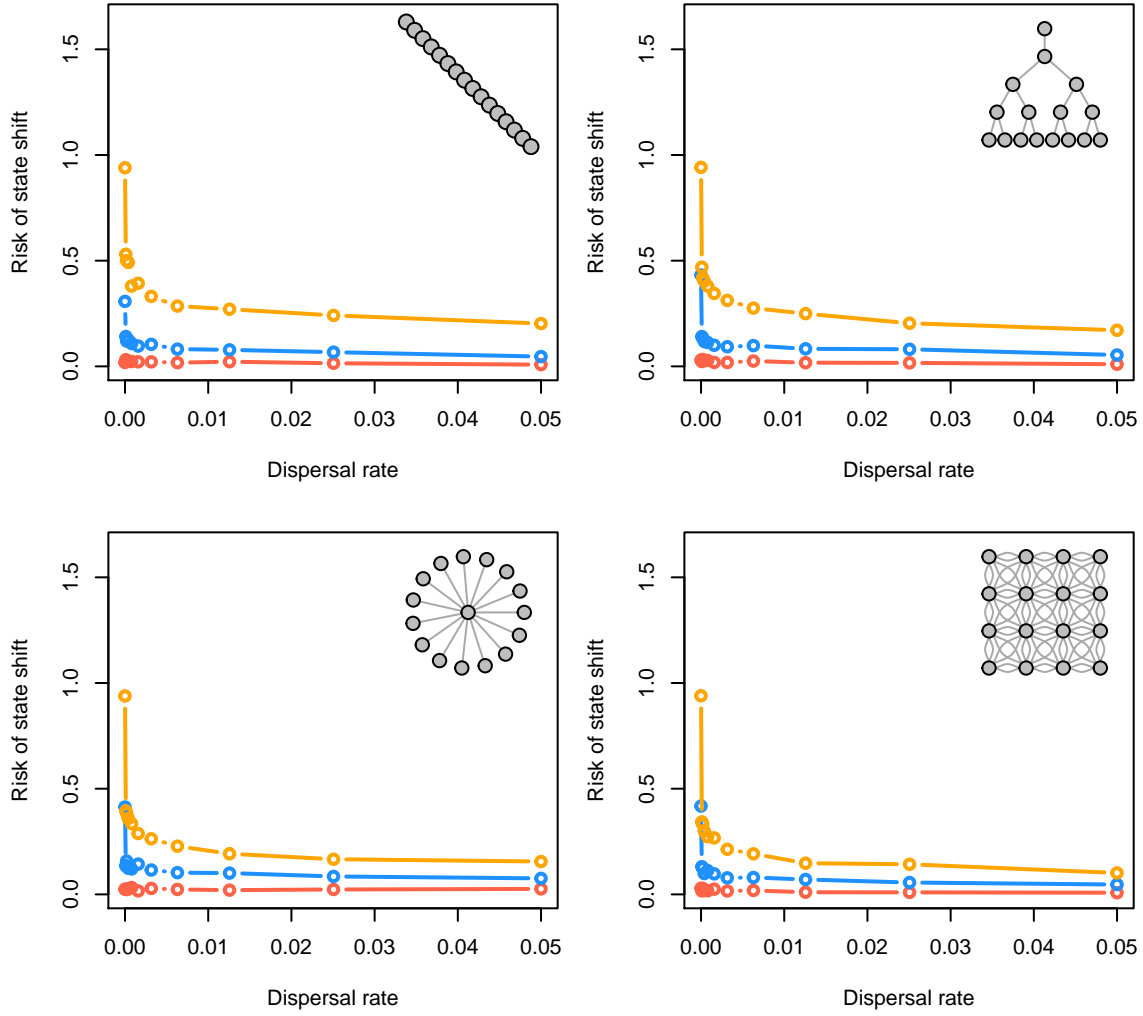


Figure S22: Risk of state shift after 100 generations along dispersal, disturbance (red - uniform; blue - localized, random; orange - localized, extirpation), and network gradients with variable patches and stochastic recruitment.

State shifts with variable patches, and spatio-temporally correlated stochasticity

Now, we illustrate how variable patch demography and high spatial-temporal correlations in stochastic recruitment affects the risk of a state shift.

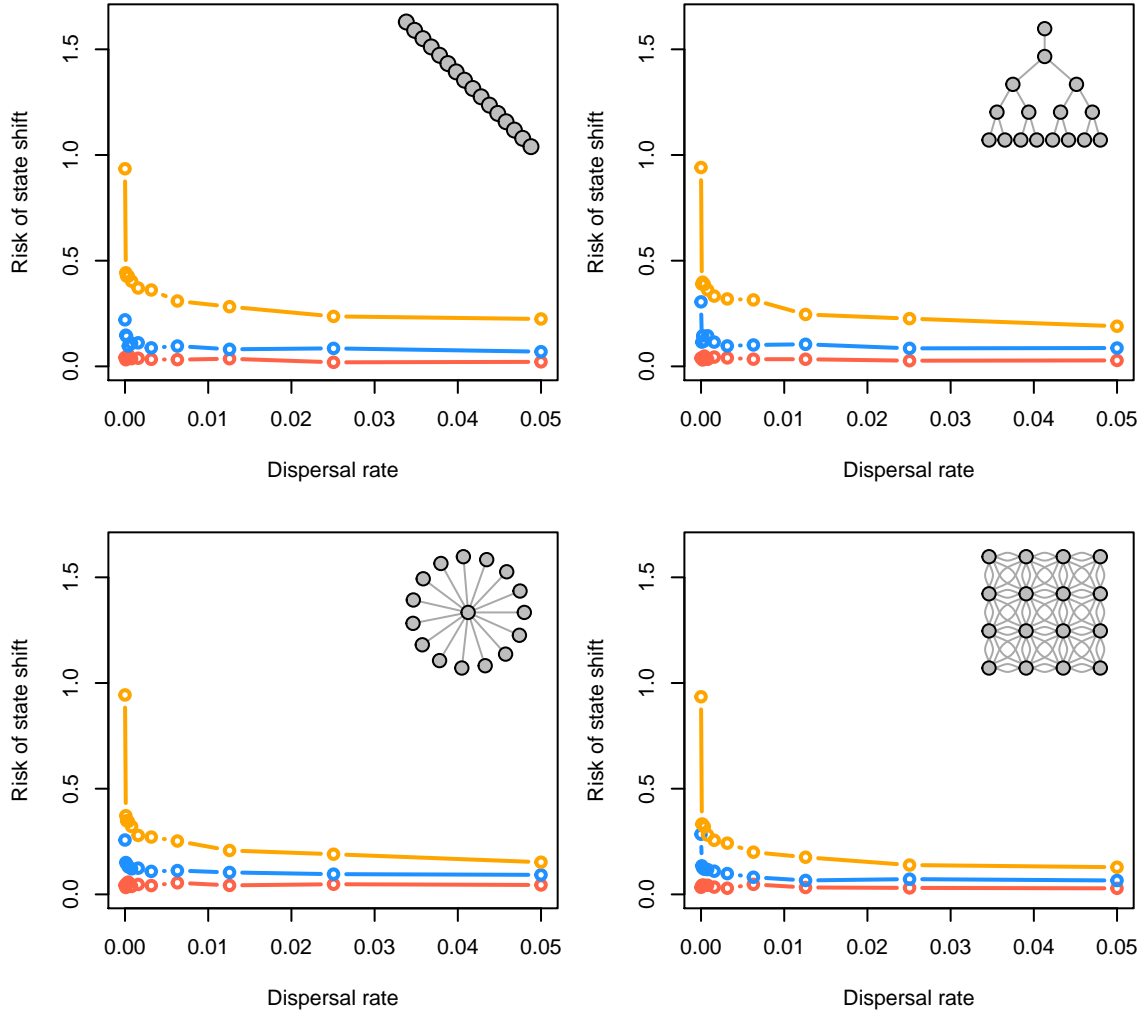


Figure S23: Risk of state shift (lack of recovery or spatial contraction) after 100 generations along dispersal, disturbance (red - uniform; blue - localized, random; orange - localized, extirpation), and network gradients with variable patches, and spatial-temporal correlations in stochastic recruitment.